

## Block Copolymer Mediated Synthesis of Dendritic Platinum Nanoparticles

Liang Wang<sup>†</sup> and Yusuke Yamauchi<sup>\*,†,‡</sup>

World Premier International (WPI) Research Center for Materials Nanoarchitectonics (MANA), National Institute for Materials Science (NIMS), Namiki 1-1, Tsukuba, Ibaraki 305-0044, Japan, and PRESTO, Japan Science and Technology Agency (JST), 5 Sanban-cho, Chiyoda, Tokyo, 102-0075, Japan

Received March 28, 2009; E-mail: Yamauchi.Yusuke@nims.go.jp

Synthesis of nanostructured Pt with controlled size and shape is of considerable interest.<sup>1</sup> Much effort has been focused on the tuning of the specific structural features of Pt nanostructures to produce Pt catalysts with high surface area, so as to achieve high catalytic performance and utilization efficiency.<sup>2</sup> It has been shown that the catalytic activity of Pt nanoparticles in the catalytic reaction between hexacyanoferrate(III) and thiosulfate ions is shape-dependent.<sup>1a</sup> Accordingly, various strategies have been developed to synthesize Pt nanostructures with different shapes, such as nanospheres,<sup>3</sup> nanowires,<sup>4</sup> mesoporous structures,<sup>5</sup> etc. Despite the above successful demonstrations, the synthesis of a new type of Pt nanostructures, e.g., dendritic Pt nanoparticles (DPNs) with a well-defined shape, is still highly desirable and technologically important. The structures of DPNs are favorable for reducing the Pt consumption, providing high surface area, and facilitating enhanced performance in catalytic applications. Very few examples of the synthesis of DPNs have been demonstrated to date<sup>6</sup> in which complicated synthesis is needed and the surface area of the product is relative low. Developing a reliable and facile strategy to finely control the nanostructure of the DPNs is an urgent topic to be solved.

Herein, a rapid, one-step, and efficient route was proposed to synthesize DPNs in high yield, which was mediated by Pluronic F127 block copolymer (PEO<sub>100</sub>PPO<sub>65</sub>PEO<sub>100</sub>) from the reduction of a Pt complex by ascorbic acid (AA) without the need for any organic solvents, direct templates, or ion replacements. Since the synthesis of Au nanoparticles mediated by block copolymer was developed,<sup>7</sup> the block copolymer mediated synthetic strategy has been successfully applied to synthesizing a few metal nanoparticles, such as Au,<sup>8</sup> Pt,<sup>9</sup> and Pd<sup>10</sup> nanoparticles. It was noted the metal nanoparticles prepared by this strategy were limited to spherical nanoparticles. The lack of sharp corners and edges devalue the advantages of metal nanoparticles, especially for Pt nanoparticles in catalytic application. The rich edges and corner atoms derived from the dendritic structure of the DPNs are highly desired for improving the catalytic performance.<sup>1a,2,6b</sup> In this regard, it would be more interesting if the block copolymer mediated synthesis could produce DPNs. In this synthesis, besides acting as a protecting agent, Pluronic F127 molecules played another important role, structure-directing agent. To the best of our knowledge, this approach is the first report on the facile synthesis of DPNs through a block copolymer mediated synthetic strategy.

To prepare the DPNs, 5 mL of 20 mM K<sub>2</sub>PtCl<sub>4</sub> aqueous solution containing 0.794 mM Pluronic F127 were placed in a small beaker and then 5 mL of 0.1 M AA were quickly added, giving final K<sub>2</sub>PtCl<sub>4</sub>, Pluronic F127, and AA concentrations of 10, 0.397, and 0.05 mM, respectively. The mixture solution was put into an

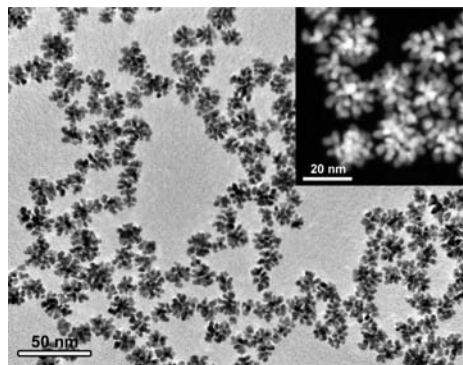


**Figure 1.** Bright-field TEM image of the DPNs. The inset image is a dark-field TEM image of the DPNs.

ordinary ultrasonic bath under a 56 kHz operating frequency for 10 min. As the Pt deposition proceeded, the color of the reaction solution was gradually changed from transparent light brownish-yellow to brown and then to opaque black (Figure S1). The Pt complex was completely reduced (Figure S2). The shape and size of the typical synthesized DPNs were characterized by TEM. Figure 1 and Figure S3A revealed the presence of abundant DPNs with a shape distribution of complete dendritic shape, demonstrating the high yield formation of the DPNs (~100%). The size of the DPNs ranged narrowly from 13 to 23 nm with an average diameter of 17.4 nm (Figure S4). The dendritic nature of the nanoparticles was more evident in the images obtained by scanning TEM using a high-angle annular dark field (HAADF) (Figure 1 Inset and Figure S3B), and each branch of the DPNs was seen to end with a rice-shaped 3–3.5 nm tip. The number of branches on each DPN differed from particle to particle, ranging from a few to over 20.

The HRTEM image of the individual DPN, shown in Figure 2, indicated the nanoparticle was a dendritic entity with branching in various directions. The lattice fringes were coherently extended across over several branches. Since the domain boundaries were clearly observable, as indicated by the arrows, the individual DPN was not single-crystalline nature. The filtered image in the square area showed the lattice fringes corresponded to {111} planes of Pt, because both *d* spacings were 0.23 nm and the dihedral angle was ~70° (Figure 2). The X-ray diffraction (XRD) pattern of the product was for the *fcc* Pt crystal structure (Figure S5) consistent with the selected area electron diffraction (SAED) pattern of the sample (Figure S3A Inset). Interestingly, the shape of the DPNs could survive to some degree after the heat annealing process at 250 °C for 2 h without evident change of their original shape, but with a little aggregation (Figure S6).

After consecutive washing/centrifugation cycles with water, the product had a nearly “clean” surface (Figure S7). The N<sub>2</sub> adsorption–desorption isotherm of the product (Figure S8) gave a surface area of 56 m<sup>2</sup> g<sup>-1</sup>, which is even higher than the reported

<sup>†</sup> WPI Research Center for MANA, NIMS.

<sup>‡</sup> PRESTO, JST.

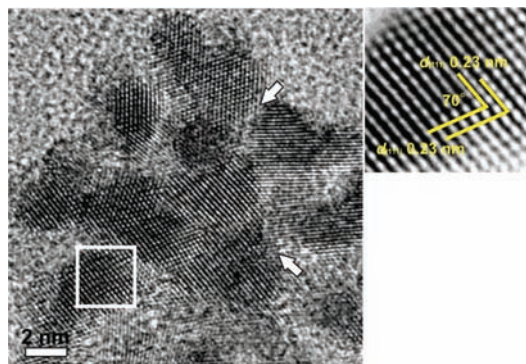


**Figure 2.** HRTEM image of one DPN (left) and filtered image of the square area (right). The domain boundaries are indicated by the arrows.

highest value  $53 \text{ m}^2 \text{ g}^{-1}$  for unsupported Pt materials.<sup>4</sup> This value is very close to the value  $57 \text{ m}^2 \text{ g}^{-1}$ , calculated roughly for the surface areas of nanowires with 3.25 nm in average diameter, indicating that the inner edge and corner area are truly accessible from outside. Such a high surface area was created from the branches with 3–3.5 nm tips. The combination of high surface area with the nanoarchitectures consisting of edges is advantageous for catalytic applications.

For comparison, the specific surface areas of Pt black range from 20 to  $28 \text{ m}^2 \text{ g}^{-1}$ .<sup>11</sup> Porous Pt nanoparticles synthesized at  $210 \text{ }^\circ\text{C}$  using a complicated organic phase showed a surface area of  $14 \text{ m}^2 \text{ g}^{-1}$ .<sup>6a</sup> Although multiarmed Pt nanostars with high catalytic activity could be prepared by using tetrahedral Pt nanocrystals as seeds, the size distribution was varied.<sup>6b</sup> Therefore, this synthetic strategy can be proposed as a more simple, rapid, and straightforward method for synthesis of DPNs with high surface areas and high yield.

To help understand the process of shape evolution in this system, two intermediate products harvested at two different times during the reaction solution kept in the brown color stage (Stage B in Figure S1), which was most likely the rapid growth period, were observed by TEM (Figure S9). As Figure S9A displayed at the earlier harvested time, AA reduced the Pt complex precursor to yield initial irregular particles with sprouts in random directions formed likely by aggregation of discrete Pt nanoparticles. As the reaction proceeded, the particle size continued to increase and secondary branches began to grow from the bodies and main branches due to the continuous precursor reduction, leading to the growth of the immature particles to a size of  $\sim 6 \text{ nm}$  at the later harvested time (Figure S9B). Such growth continuously occurred as the reaction proceeded until complete consumption of the Pt precursor in the reaction solution. At  $\sim 10 \text{ min}$ , the color of the reaction color remained stable opaque black, suggesting that the reaction was complete, and the mature structures of the nanoparticles were obtained (Figure 1). This type of crystal growth was previously observed for the formation of hyperbranched Ag nanostructures.<sup>12</sup>

To understand the role of Pluronic F127 in this system, investigations were done by replacing Pluronic F127 with different surfactants (Figure S10). Based on these investigations, it was known that Pluronic surfactants were critical for the formation of the DPNs shown in Figure 1. It was reasonable to speculate about Pluronic F127 molecules serving as a structure-directing agent in this system. The PEO group in PEO–PPO–PEO surfactants

(Pluronic surfactants) was known to form a crown-ethers-like conformation, similar to a cavity structure in aqueous solution.<sup>7a</sup> The hydrophobic PPO groups in the Pluronic polymer were favorably adsorbed onto the surface of the deposited metal surface.<sup>7,9</sup> The Pluronic chains adsorbed on the Pt surface during the Pt deposition in this system could form cavities and then facilitate the formation of the DPNs. It was worth noting that the used Pluronic F127 concentration was lower than its critical micelle concentration (CMC).<sup>7a,b</sup> Ill-defined DPNs were produced by using a Pluronic F127 concentration over its CMC (Figure S11). Over CMC, the PPO groups existed in the core of the micelles and the hydrophilic PEO groups were exposed on the micelles. Therefore, the PPO groups could not effectively adsorb on the Pt surface during the Pt deposition, which was unfavorable for dendritic growth. Under the current system, a low Pt concentration (1 mM) resulted in irregular nanoparticles (Figure S12A) and relatively higher Pt precursor concentrations were favorable for facilitating the production of DPNs in high yield and high quality (Figure S12B–D).

In summary, DPNs were straightforwardly synthesized in high yield via a one-step aqueous-phase reaction mediated by block copolymer under mild conditions. The proposed method was unique in its simplicity. As-prepared DPNs possessed the highest surface area of all reported unsupported Pt materials. Traditionally, block copolymers could be utilized as direct templates for synthesis of silica-<sup>13</sup> and metal-based<sup>5</sup> mesoporous materials. The proposed block copolymer mediated synthesis might open a new door toward creation of novel metal-based dendritic materials. We expect that this synthetic concept could be a new bridge between two frontline disciplines: block copolymer systems and dendritic metal design.

**Acknowledgment.** This work was supported by WPI, MEXT of Japan and partially supported by a Grant-in-Aid for Scientific Research (No. 19850031) from JSPS and the Murata Science Foundation.

**Supporting Information Available:** Preparation process, additional TEM and photo images, EDX, XRD, SAED, and  $\text{N}_2$  adsorption/desorption isotherm data. This material is available free of charge via the Internet at <http://pubs.acs.org>.

## References

- (1) (a) Narayanan, R.; El-Sayed, M. A. *Nano Lett.* **2004**, *4*, 1343. (b) Song, Y.; Yang, Y.; Medforth, C. J.; Pereira, E.; Singh, A. K.; Xu, H.; Jiang, Y.; Brinker, C. J.; Swol, F.; Shelnut, J. A. *J. Am. Chem. Soc.* **2004**, *126*, 635.
- (2) Lim, B.; Lu, X. M.; Jiang, M. J.; Camargo, P. H. C.; Cho, E. C.; Lee, E. P.; Xia, Y. N. *Nano Lett.* **2008**, *8*, 4043.
- (3) Bigall, N. C.; Hartling, T.; Klose, M.; Simon, P.; Eng, L. M.; Eychmuller, A. *Nano Lett.* **2008**, *8*, 4588.
- (4) Song, Y. J.; Garcia, R. M.; Dorin, R. M.; Wang, H. R.; Qiu, Y.; Coker, E. N.; Steen, W. A.; Miller, J. E.; Shelnut, J. A. *Nano Lett.* **2007**, *7*, 3650.
- (5) Yamauchi, Y.; Takai, A.; Nagaura, T.; Inoue, S.; Kuroda, K. *J. Am. Chem. Soc.* **2008**, *130*, 5426.
- (6) (a) Teng, X. W.; Liang, X. Y.; Maksimuk, S.; Yang, H. *Small* **2006**, *2*, 249. (b) Mahmoud, M. A.; Tabor, C. E.; El-Sayed, M. A.; Ding, Y.; Wang, Z. L. *J. Am. Chem. Soc.* **2008**, *130*, 4590.
- (7) (a) Sakai, T.; Alexandridis, P. *J. Phys. Chem. B* **2005**, *109*, 7766. (b) Sakai, T.; Alexandridis, P. *Langmuir* **2004**, *20*, 8426. (c) Sakai, T.; Alexandridis, P. *Langmuir* **2005**, *21*, 8019.
- (8) Wang, X. G.; Kawanami, H.; Islam, N. M.; Chatterjee, M.; Yokoyama, T.; Ikushima, Y. *Chem. Commun.* **2008**, 4442.
- (9) Niesz, K.; Grass, M.; Somorjai, G. A. *Nano Lett.* **2005**, *5*, 2238.
- (10) Meier, M. A. R.; Filali, M.; Gohy, J.; Schubert, U. S. *J. Mater. Chem.* **2006**, *16*, 3001.
- (11) Choi, K. S.; McFarland, E. W.; Stucky, G. D. *Adv. Mater.* **2003**, *15*, 2018.
- (12) Wang, Y. L.; Camargo, P. H. C.; Skrabalak, S. E.; Gu, H. C.; Xia, Y. N. *Langmuir* **2008**, *24*, 12042.
- (13) Wan, Y.; Zhao, D. Y. *Chem. Rev.* **2007**, *107*, 2821.

JA902485X